Original Paper

Effects of crystal diameter and heat reservoir on the growth of Ce:$Gd_3(Al, Ga)_5O_{12}$ crystals using the infrared convergent heating floating zone method

Md. Zahid HASAN[1], Satoshi WATAUCHI[1*], Yuki MARUYAMA[1], Masanori NAGAO[1], Shunsuke KUROSAWA[2,3], Yuui YOKOTA[4], Akira YOSHIKAWA[2,4,5], Isao TANAKA[1]

[1]Center for Crystal Science and Technology, University of Yamanashi, 7-32 Miyamae, Kofu, Yamanashi 400-0021
[2]New Industry Creation Hatchery Center (NICHe), Tohoku University, 6-6-10 Aoba, Aramaki, Aoba-ku, Sendai, Miyagi 980-8579
[3]Department of Physics, Yamagata University, 1-4-12 Kojirakawa-machi, Yamagata 990-8560
[4]Institute for Materials Research, Tohoku University, 2-1-1 Katahira, Aoba-ku, Sendai, Miyagi 980-8577
[5]C&A Corporation, 1-15-9 Ichibancho, Aoba-ku, Sendai, Miyagi, 980-0811

Received June 16, 2020; E-mail: watauchi@yamanashi.ac.jp

Cerium-doped $Gd_3(Al,Ga)_5O_{12}$ (GAGG:Ce) crystals were grown using the infrared convergent heating floating zone (IR-FZ) method. As the grown crystals contained many cracks, growth conditions were optimized to reduce them and the effects of crystal diameter and heat reservoir were examined. The crystal diameter was controlled by the feed diameter. No clear effect of the heat reservoir was observed on crystals grown 9 mm in diameter, and the crystals contained many cracks despite using the heat reservoir. However, clear suppression effects were observed in crystals grown 15 mm in diameter using the heat reservoir. It was determined that not only the heat reservoir, but also the crystal diameter (controlled by the feed diameter) affected the formation of the cracks in the grown crystal. The temperature distribution was also measured in the different heat reservoir conditions using a virtual sample with different diameter. The temperature gradient was also affected by both the virtual sample size and the presence of the heat reservoir.

Key Words: *Floating zone method, Heat reservoir, Crystal diameter, Grain size, Temperature distribution*

1. Introduction

Detectors for high-energy photons and particles consist of scintillation materials and photomultiplier tubes, which have various applications in X-ray computed tomography (CT), positron emission tomography (PET), and high-energy physics detectors [1,2]. A Cerium-doped $Gd_3Al_2Ga_3O_{12}$ (GAGG:Ce) crystal is a promising inorganic scintillator for X-rays and γ-rays [2-5], because it has a high light yield of approximately 46,000 photon/MeV and an excellent energy resolution of 3.7%@662 keV [6]. It is also non-hygroscopic in nature.

Crystals of GAGG:Ce have previously been grown using various techniques, such as the Czochralski method (CZ) [2], the micro-pulling-down (μ-PD) method [3], and the infrared convergent floating zone (IR-FZ) method [7]. In the CZ and the μ-PD methods except the IR-FZ method, iridium crucibles are necessary for crystal growth. Therefore, the growth atmosphere is limited to an oxygen atmosphere of less than ~2 % [2]. In the IR-FZ method, on the other hand, various atmospheric conditions, including a higher amount of oxygen in the growth atmosphere, can be applied [7]. The highest light yield was achieved with crystals grown in a 100% O_2 gas condition [7]; however, the diameter of the grown crystal was only 4 mm, which is too small to be practical in real-life manufacturing methods, and the grown crystal contained many cracks.

Some coauthors of this paper have improved the diameter of the crystal grown by the IR-FZ method using a tilting angle and position effects of mirror-lamp (M-L) systems for the growth of rutile and silicon crystals [8-11]. Kitamura *et al*. [12] reported that a heat reservoir was effective in suppressing crack formation in a $Y_3Al_5O_{12}$ (YAG) crystal grown by the IR-FZ method. The temperature distribution along the vertical direction was also measured by a thermocouple directly. The temperature gradient was significantly reduced, from 430 °C/cm to 85-140 °C/cm, at the grown crystal area by inserting the heat reservoir, which is 1 cm below the focus [12]. But the effects of the radiation would be dominant in this measurement condition.

In this study, therefore, we attempted to grow larger diameter GAGG:Ce crystals using the IR-FZ method and reduce crack formation in the crystal using the effects of a heat reservoir. Then the temperature distributions around the convergent area was also measured in the condition that an alumina tube was set at the convergent area as a virtual sample to account for the effects of the thermal conductivity of the vertical sample on the temperature distribution.

2. Experimental

2.1 Crystal growth

High-purity Gd_2O_3 (99.99%), β-Ga_2O_3 (99.99%), α-Al_2O_3 (99.99%), and CeO_2 (99.99%) were used as starting materials. Appropriate amounts of these materials, to obtain $(Gd_{0.998}Ce_{0.002})_3Ga_2Al_3O_{12}$, were weighed out and mixed with ethanol. The mixed powder was calcined at 1300 °C for 10 h in air. The calcined powder was placed in a rubber tube to form a rod shape. The rods were pressed up to 300 MPa using a cold isostatic pressing machine (Nikkiso Co. Ltd.: Model CL3-22-60). A pressed rod was used as a feed rod for the IR-FZ growth. The feed preparation process is similar to that used in reported IR-FZ growth methods [7]. In this experiment, as-pressed feeds with various diameters, ranging from 10 mm to 19 mm, were used for the growth experiments without sintering. The typical length of these feeds in our growth experiments, was ~80 mm. A polycrystalline rod was used as the seed rod. A four-ellipsoidal mirror-type infrared convergent furnace (Crystal Systems Corporation: model FZ-T-10000-H-TY-1) was used for crystal growth. Four halogen lamps, with rated outputs of 1.5 kW, were used

as heat sources, because the melting point of GAGG:Ce is approximately 1850 °C, which is similar to that of rutile. The total rated lamp output of the furnace was 6.0 (1.5 × 4) kW. In this experiment, the crystals were grown with and without the heat reservoir positioned at the grown crystal area to investigate the effects of the heat reservoir. The size of the alumina tube inserted at the grown crystal area as a heat reservoir, was 42 mm in the outer diameter and 35 mm in the inner diameter, respectively. Fig.1 shows a schematic illustration of the experimental setup with the heat reservoir inserted. The major growth conditions are summarized in Table I. The effects of both the feed size and the heat reservoir on crack formation in the GAGG:Ce crystals, grown by the IR-FZ method, were investigated. As shown in Table I, the diameter of the grown crystal was controlled by the feed diameter because the constant moving rates were applied for both the upper and lower shafts through this experiment. Some of the grown crystals were cut along the growth direction to observe the cut surface. The number of grains on each cut surface was counted for characterization. The orientations of a few grains were checked by the back-reflection Laue X-ray diffraction (XRD).

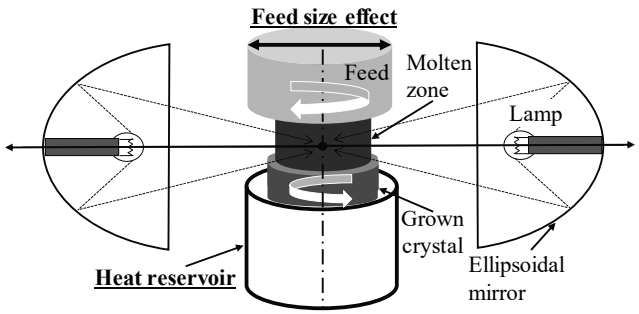

Fig.1 Schematic illustration of the experimental setup. The feed size and heat reservoir effects were examined.

Table I Typical growth conditions for GAGG:Ce crystals

Feed diameter (mm)	10, 13, 16, 19
Heat reservoir	Insert / Non-insert
Rotation rate (upper / lower) (rpm)	2/45
Shaft moving rate (upper / lower) (mm/h)	6.8/5.0
Growth atmosphere	O_2 flow 200 mL/min

2.2 Temperature distribution measurement

Fig.2 shows the experimental setup for the temperature distribution measurement. The furnace and the lamps as heat sources used for the temperature distribution measurement were the same as those used for crystal growth. Fig.2(a) shows the normal crystal growth conditions when the heat reservoir is not inserted. Fig.2(b) depicts the crystal growth conditions when the heat reservoir is inserted. In both cases, an alumina tube was set along the rotational axes of the upper and lower shafts as a virtual sample. To investigate the diameter effects of the virtual sample on the temperature distribution, alumina tubes with two different sizes were used. One was a tube with an outer diameter of 10 mm and an inner diameter of 5 mm and the other was a tube with an outer diameter of 15 mm and an inner diameter of 10 mm. The type R thermocouple, with a 0.5 mm diameter, connected to a digital multimeter via extension lead wires was placed inside the virtual sample tube with an alumina thermocouple ceramic insulator to measure the temperature distribution along the vertical line. Fig.2(b) shows the way in which another large alumina tube was placed as a heat reservoir in addition to the alumina tube acting as a virtual sample. The heat reservoir alumina tube is the same as that used for the growth of GAGG:Ce crystals.

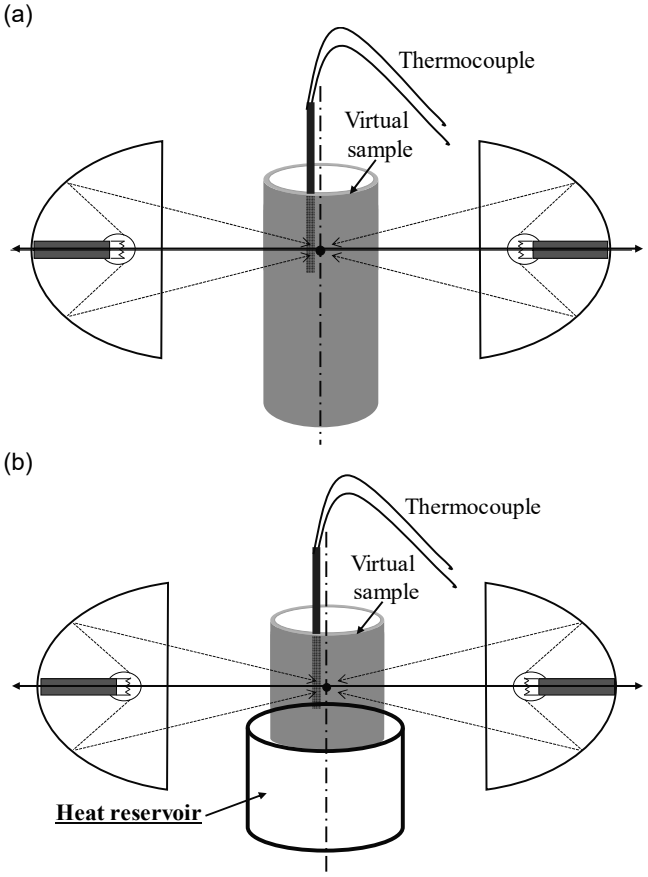

Fig.2 Schematic illustrations of temperature distribution measurements. An alumina tube, 10 mm in outer diameter, was used as a virtual sample. The temperature distribution in the tube was measured by a thermocouple along the vertical direction in the absence of a heat reservoir, a large alumina tube with a 42 mm outer diameter (a). A large alumina tube was placed as a heat reservoir (b).

3. Results and Discussion

3.1 Crystal experiment

Fig.3 shows images of the Ce 0.2 at% doped GAGG crystals grown by using different feed rods with and without a heat reservoir. Fig.3(a), (b), (c), and (d) show the GAGG:Ce crystals grown without a heat reservoir using feed rods of 10 mm, 13 mm, 16 mm, and 19 mm in diameter, respectively. The maximum diameters of the grown crystals were 9 mm, 12 mm, 15 mm, and 17 mm, respectively. Fig.3(e), (f), and (g) show the GAGG:Ce crystals grown with a heat reservoir using feed rods of 10 mm, 13 mm, and 16 mm in diameter, respectively. The maximum diameters of the grown crystals were 9 mm, 12 mm, and 15 mm, respectively. Most of crystals had cylindrical shapes, except for the crystals shown in Fig.3(d) and (g), which had conical shapes. In all of these growths, the required lamp power increased with progressive crystal growth. In the growth of the crystals shown in Fig.3(d) and (g), the required lamp achieved full power. The practical feeding rate had to be reduced during the crystal growth by lifting up the feed rod frequently to avoid contact of the feed with the grown crystal, which caused the conical shapes. Therefore, for these two crystals, the crystal diameters were defined at the initial parts of the grown crystals. All the crystals were yellowish in color and contained cracks. The formation was not so

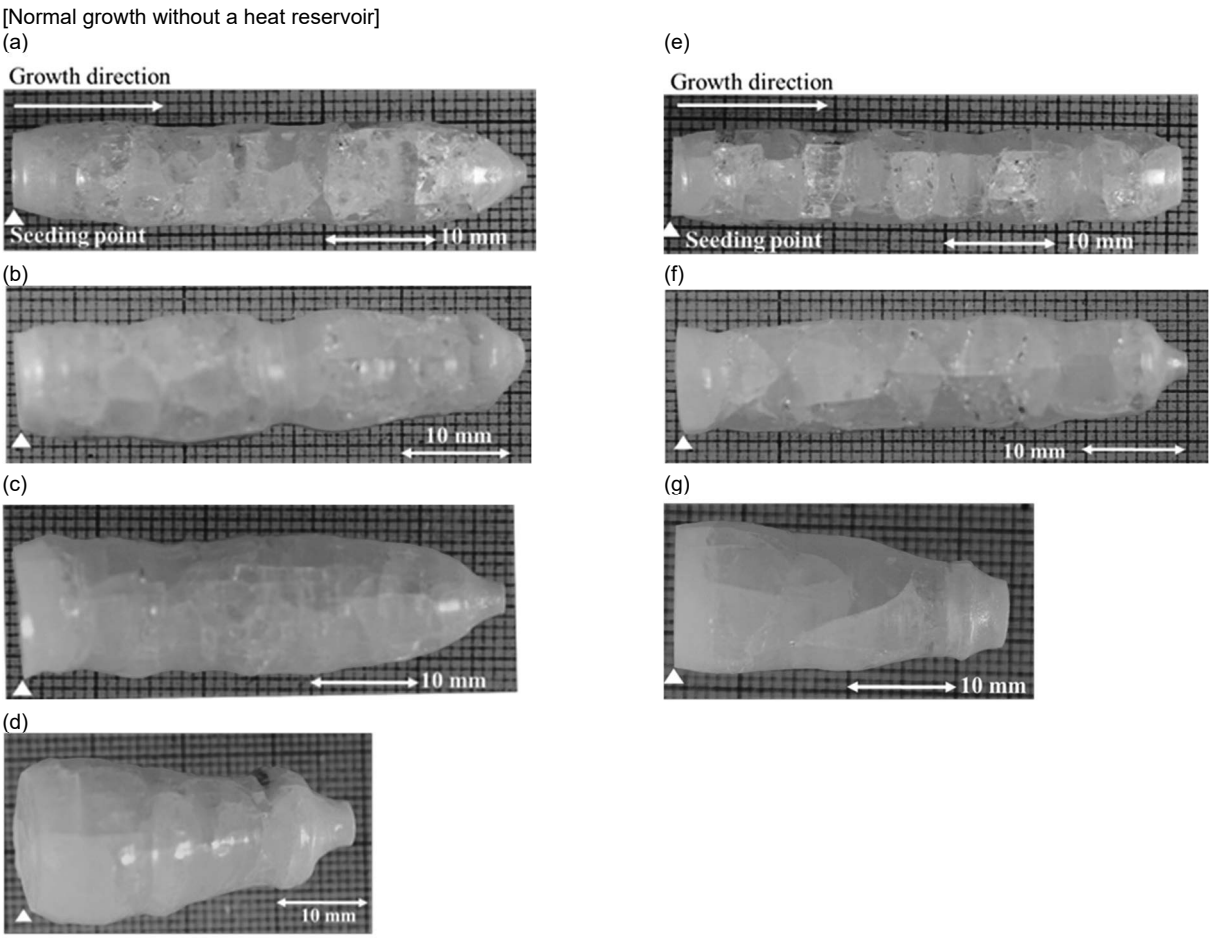

Fig.3 Ce 0.2 at% doped GAGG crystals grown without a heat reservoir using feed rods of (a) 10 mm, (b) 13 mm, (c) 16 mm, (d) 19 mm in diameter, and with a heat reservoir using feed rods of (e) 10 mm, (f) 13 mm, and (g) 16 mm in diameter.

affected by the use of the single crystalline seeds in our limited trial growth along <100> as shown in supplemental figures. In this case, cracks were formed even in the single crystalline seed. Therefore, all these crystals shown in Fig.3 were grown using a polycrystalline seed.

Fig.4(a) and (b) show snapshots of the molten zone area during crystal growth for both the normal growth conditions (without the heat reservoir) and the conditions where the heat reservoir is inserted. In both cases, the diameter of the feeds was 10 mm. The molten zones were stable and the cracks appeared free in the grown crystals just below the molten zone. However, the grown crystals contained many cracks at room temperature, as shown in Fig.3(a) and (e). Therefore, some of cracks were expected be formed during the cooling process. These grown crystals would be treated as polycrystals because they contain many cracks at the room temperature.

Fig.5 show the photo of the sliced sample of Fig.3(g) and the observation of the crystallographic orientations by the Laue patterns. The crystallographic orientations were found to be the same not only in the same grains but also in the adjacent grains. Although the orientations for all grains were not examined, this result supports that many curved cracks were formed during the cooling process. The

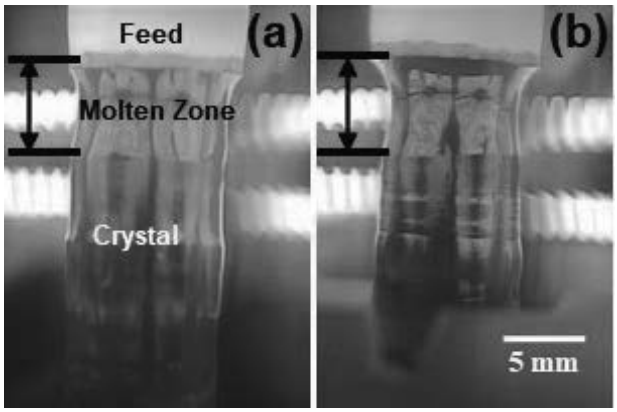

Fig.4 Snap shots of the molten zone areas during the IR-FZ growth. (a) without heat reservoir. (b) with heat reservoir.

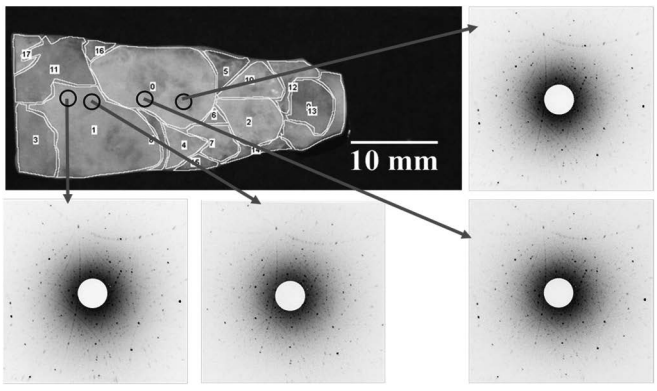

Fig.5 Laue X-ray diffraction images observed on the various surface position of the sliced sample of the crystal grown with the heat reservoir using feed rod of 16 mm in diameter.

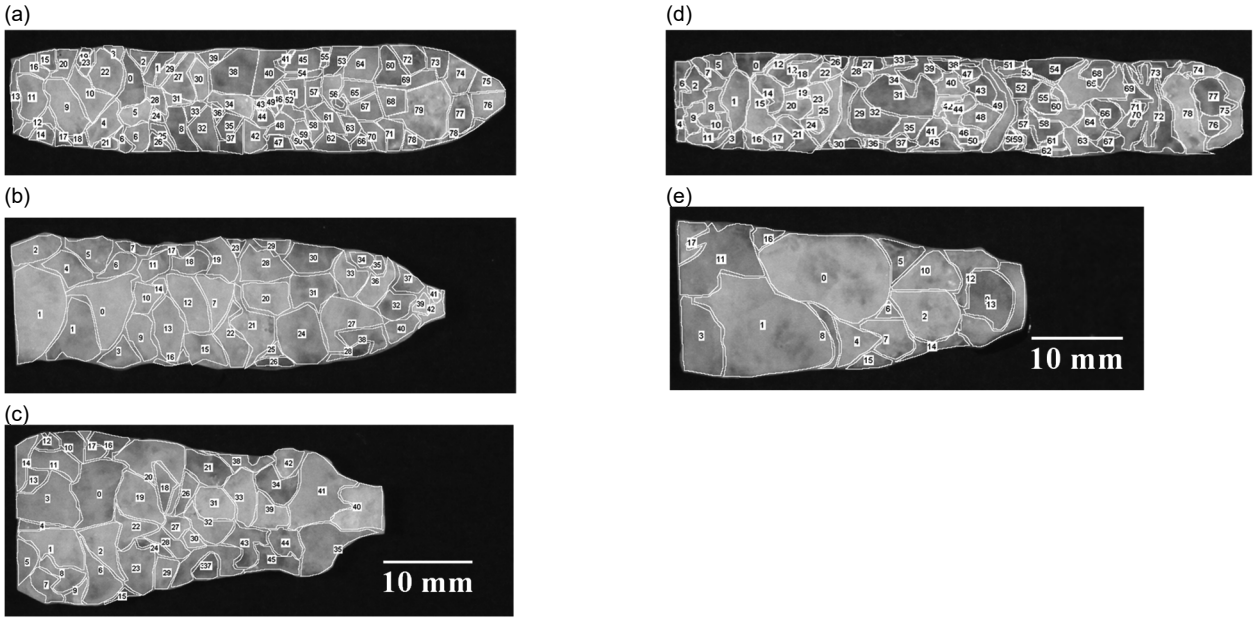

Fig.6 Sliced samples of Ce 0.2 at% doped GAGG crystals grown without the heat reservoir using feed rods of (a) 10 mm (b) 16 mm (c) 19 mm in diameter. and with the heat reservoir using feed rods of (d) 10 mm (e) 16 mm in diameter.

formation of curved cracks is also reported even in the GAGG:Ce crystals grown by the CZ method [13]. Recently, the cracks were suppressed by optimizing the cooling stage after the growth in a 4-inch diameter GAGG:Ce crystal [14].

Fig.6 shows the samples of the GAGG:Ce crystals sliced along the growth direction. Fig.6(a), (b), and (c) show samples of the 9 mm, 15 mm, and 17 mm diameter crystals grown without a heat reservoir, respectively. Fig.6(d) and (e) show the 9 mm and 15 mm diameter crystals grown in the heat reservoir. Some pieces were separated from the grown crystal boule during the slicing process.

The number of grains in each sample was counted using the Scion Image software, a free image processing software package. The area of the cross-section was also measured by the software. The average grain sizes, obtained by the square root of the cross-section area per grain, were 2.2 mm for Fig.6(a) and 2.2 mm for Fig.6(d), respectively. Although the grain sizes can be affected by the quality of the seed crystal and presence or absence of the preferential growth, the preferred growth direction was not known in GAGG:Ce and the quality of the seed was not so different because a polycrystalline rod was used as a seed through all growth experiments. The average grain size for the crystal of 9 mm diameter was independent of the presence of the heat reservoir. Conversely, the number of grains in the 15 mm diameter crystal was affected by the presence of the heat reservoir. The average grain sizes were 3.4 mm and 4.9 mm for the samples shown in Fig.6(b) and (e). The average grain size for the crystal of 17 mm diameter was 3.2 mm for the samples shown in Fig.6(c). The average grain size was plotted as a function of the crystal diameter, as shown in Fig.7. For both growth conditions with and without the heat reservoir, the average grain size increased with the crystal diameter. The crystal volume is proportional to the square of the crystal diameter, and the size of the side surface area is proportional to the diameter if the growth length is constant. We can assume that the volume is related to the heat capacity and that the side surface area is related to the dissipation of heat by radiation. Therefore, the thermal conditions of the crystal can be affected by the diameter. However, further improvements were not recognized in the 17 mm diameter crystal, which may indicate limitations to the diameter effects on the average grain size. Making use of the heat reservoir, no clear effect on the average grain size was observed for the crystal with a diameter of 9 mm, however, clear effects were observed for the 15 mm diameter crystal. In the 15 mm diameter crystal, the distance between the periphery of the grown crystal and the inner wall of the heat reservoir is shorter than that for the 9 mm diameter crystal. This distance may be important in the appearance of heat reservoir effects. At least we can say that the combination effects of the crystal size and the heat reservoir are important than each individual effect for the crack formation related to the cooling process.

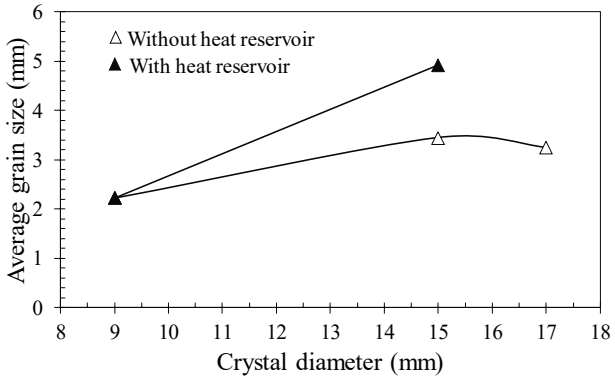

Fig.7 The average grain size as a function of the crystal diameter.

3.2 Temperature distribution measurement

Fig.8 shows the temperature distributions of the inner wall of the alumina tube, set as a virtual sample (depicted in Fig.2). The zero position on the vertical axis of Fig.8 describes the position where the highest temperature reached. Fig.8(a) and (b) are the temperature distributions for vertical samples of 10 mm and 15 mm in outer diameter, respectively. In each figure, both temperature distributions measured without and with heat reservoir conditions were shown. The applied lamp power was changed to achieve the highest temperature of ~1560 °C. The achieved highest temperature was in the range from 1551 °C to 1569 °C. The temperature distributions for minus vertical positional area (grown crystal area) were broadened by inserting the heat reservoir and by using the larger virtual sample in outer diameter.

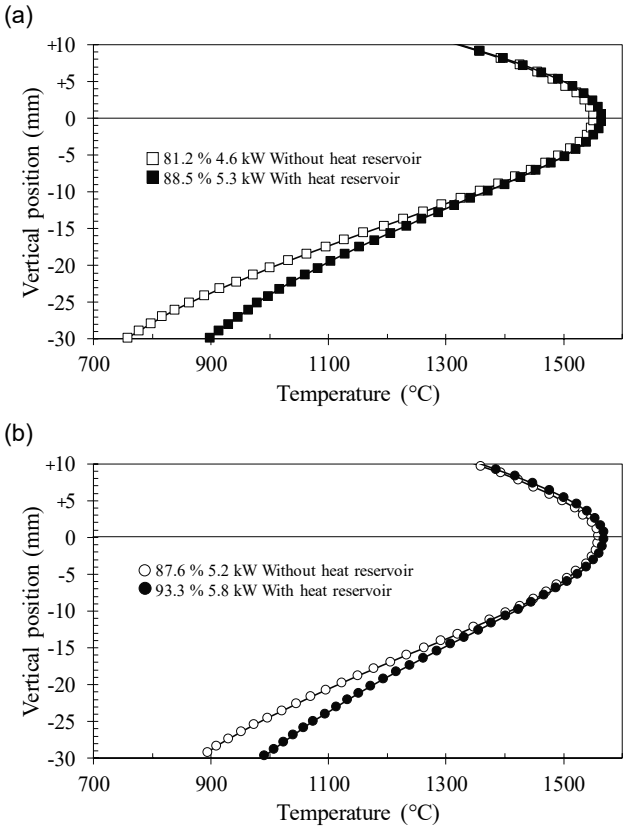

Fig.8 Temperature distribution of the inner wall of the alumina tubes with outer diameter of (a) 10 mm (b) 15 mm set as a virtual sample.

Kitamura *et al*. reported that the temperature gradient was significantly reduced, from 430 °C/cm to 85-140 °C/cm, at the grown crystal area by inserting the heat reservoir when the temperature was measured directly by the thermocouple without a virtual sample using a double-ellipsoidal mirror-type furnace [12]. Therefore, the values of the temperature gradient at the grown crystal area were also calculated numerically. Fig.9 shows the maximum temperature gradient for each temperature distribution as a function of the outer diameter of the virtual sample. The vertical positions of the maximum temperature gradient, ranging from -16 mm to -10 mm, were dependent on each measurement. The maximum value of the temperature gradient decreased with the increase of the outer

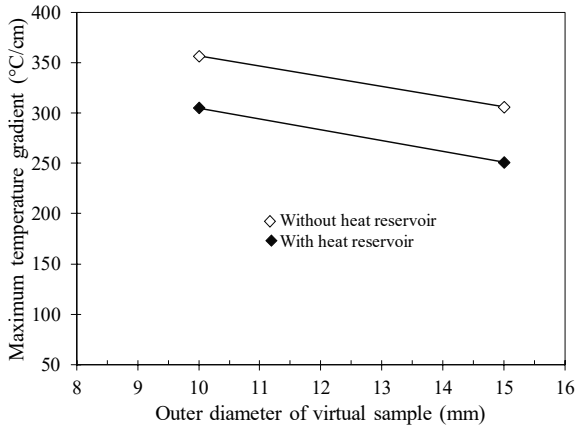

Fig.9 Maximum temperature gradient as a function of the outer diameter of the virtual sample.

diameter of the virtual sample and by the use of the heat reservoir. This means that the cooling process of the grown crystal can be affected by both the virtual sample size and the presence of the heat reservoir.

This behavior was consistent with the formation of cracks shown in Fig.6. The crack formation tended to be reduced in the condition that the maximum temperature gradient was lower. The maximum temperature gradient for virtual sample with 15 mm in outer diameter was 250 °C/cm using a four-ellipsoidal mirror-type furnace in our experiment, which is still larger than 85-140 °C/cm reported by Kitamura et al. using a double-ellipsoidal mirror-type furnace [12]. We may have to explore the growth condition to realize the smaller temperature gradient. At least we can say that not only the presence of the heat reservoir but also the outer diameter of the virtual sample affects the temperature distribution.

4. Conclusions

The effects of the crystal diameter and the heat reservoir on the growth of GAGG:Ce crystals by the floating zone method using infrared convergent heating were studied. Although the effects of the heat reservoir were not clear when growing a 9 mm diameter crystal using a 10 mm diameter feed rod, they were clear when growing a 15 mm diameter crystal using a 16 mm diameter feed rod. Based on the average grain size on the sliced surfaces of the grown crystals, both the heat reservoir and the diameter of the crystal affect the formation of the cracks. The temperature distribution and the temperature gradient were also affected not only by the heat reservoir, but also the virtual sample size.

Acknowledgement

This work was partially supported by the GIMRT Program of the Institute for Materials Research, Tohoku University.

References

1) A. Yoshikawa, K. Kamada, S. Kurosawa, Y. Shoji, Y. Yokota, V.I. Chani, M. Nikl, *J. Lumin.*, **2016**, *169*, 387.
2) K. Kamada, T. Yanagida, T. Endo, K. Tsutumi, Y. Usuki, M. Nikl, Y. Fujimoto, A. Fukabori, A. Yoshikawa, *J. Cryst. Growth*, **2012**, *352*, 88.
3) K. Kamada, T. Endo, K. Tsutumi, T. Yanagida, Y. Fujimoto, A. Fukabori, A. Yoshikawa, J. Pejchal, M. Nikl, *Cryst. Growth Des.*, **2011**, *11*, 4484.
4) K. Kamada, T. Yanagida, J. Pejchal, M. Nikl, T. Endo, K. Tsutumi, Y. Fujimoto, A. Fukabori, A. Yoshikawa, *J. Phys. D: Appl., Phys.*, **2011**, *44*, 505104.
5) B. Seitz, N. Campos Rivera, A. G. Stewar, *IEEE Trans. Nucle. Sci.*, **2016**, *63*, 503.
6) P. Sibczynskia, J. Iwanowska-Hanke, M. Moszyński, L. Swiderski, M. Szawłowski, M. Grodzicka, T. Szczęśniak, K. Kamada, A. Yoshikawa, *Nucle. Instr. Meth. Phys. Res. A*, **2015**, *772*, 112.
7) A. Yoshikawa, Y. Fujimoto, A. Yamaji, S. Kurosawa, J. Pejchal, M. Sugiyama, S. Wakahara, Y. Futami, Y. Yokota, K. Kamada, K. Yubuta, T. Shishido, M. Nikl, *Opt. Mater.*, **2013**, *35*, 1882.
8) S. Watauchi, M. A. R. Sarker, M. Nagao, I. Tanaka, T. Watanabe, I. Shindo, *J. Cryst. Growth*, **2012**, *360*, 105.
9) M. A. R. Sarker, S. Watauchi, M. Nagao, T. Watanabe, I. Shindo, I. Tanaka, *J. Cryst. Growth*, **2011**, *317*, 135.
10) M. M. Hossain, S. Watauchi, M. Nagao, I. Tanaka, *J. Cryst. Growth*, **2016**, *433*, 24.
11) M. A. R. Sarker, S. Watauchi, M. Nagao, T. Watanabe, I. Shindo, I. Tanaka, *J. Cryst. Growth,* **2010**, *312*, 2008.
12) K. Kitamura, S. Kimura, K. Watanabe, *J. Cryst. Growth*, **1982**, *57*, 475.

13) K. Kamada, Y. Shoji, V. V. Kochurikhin, S. Okumura, S. Yamamoto, A. Nagura, J. Y. Yeom, S. Kurosawa, Y. Yokota, Y. Ohashi, M. Nikl, A. Yoshikawa, *J. Cryst. Growth*, **2016**, *452*, 81.

14) V. Kochurikhin, K. Kamada, K.J. Kim, M. Ivanov, L. Gushchina, Y. Shoji, M. Yoshino, A. Yoshikawa, *J. Cryst. Growth*, **2020**, *531*, 125384.